ONCOIMMUNOLOGY
2022, VOL. 11, NO. 1, e2052418 (16 pages)
https://doi.org/10.1080/2162402X.2022.2052418

Taylor & Francis
Taylor & Francis Group

ORIGINAL RESEARCH

OPEN ACCESS Check for updates

Neutrophil extracellular traps induce tumor metastasis through dual effects on cancer and endothelial cells

Ze-Zhou Jiang[a,b], Zhi-Peng Peng[a], Xing-Chen Liu[a], Hao-Fan Guo[a], Meng-Meng Zhou[a], Da Jiang[a], Wan-Ru Ning[a], Yu-Fan Huang[a], Limin Zheng[a,b*], and Yan Wu[a*]

[a]Guangdong Province Key Laboratory of Pharmaceutical Functional Genes, Moe Key Laboratory of Gene Function and Regulation, School of Life Sciences, Sun Yat-sen University, Guangzhou, P. R. China; [b]State Key Laboratory of Oncology in Southern China, Collaborative Innovation Center for Cancer Medicine, Sun Yat-sen University Cancer Center, Guangzhou, P. R. China

ABSTRACT

Neutrophils constitute a major component in human hepatocellular carcinoma (HCC) and can facilitate disease progression via poorly understood mechanisms. Here, we show that neutrophil extracellular traps (NETs) formation was increased in human HCC tumor tissues than in paired non-tumor liver tissues. Mechanism study revealed that tumor-induced metabolic switch toward glycolysis and pentose phosphate pathway in tumor infiltrating neutrophils promoted NETs formation in a reactive oxygen species dependent-manner. NETs subsequently induced the migration of cancer cells and down-regulation of tight junction molecules on adjacent endothelial cells, thus facilitating tumor intravasation and metastasis. Accordingly, NETs depletion could inhibit tumor metastasis in mice *in vivo*, and the infiltration levels of NETs-releasing neutrophils were negatively associated with patient survival and positively correlated with tumor metastasis potential of HCC patients. Our results unveiled a pro-metastatic role of NETs in the milieu of human HCC, and pointed to the importance of metabolic reprogramming in shaping their characteristics, thus providing an applicable efficient target for anti-cancer therapies.

ARTICLE HISTORY
Received 14 November 2021
Revised 8 March 2022
Accepted 8 March 2022

KEYWORDS
Neutrophils; neutrophil-extracellular traps; hepatocellular carcinoma; metabolic switch; tumor metastasis

Introduction

Neutrophil extracellular traps (NETs) are aggregates released from neutrophils with DNA as a backbone and diverse molecules associated or not associated with the backbone.[1] Various stimuli, such as phorbol myristate acetate (PMA), lipopolysaccharide (LPS), interleukin 8 (IL-8), or microorganisms and their products,[1–3] could stimulate the release of NETs with extensive webs of DNA coated with citrullinated histones (Cit-H3, a NETs marker) and microbicidal proteases, such as proteinase 3 (PR3), neutrophil elastase (NE) and myeloperoxidase (MPO).[4,5] A prerequisite of NETs release is the modification of histone arginine residues to citrulline residues by protein arginine deiminase 4 (PAD4), causing massive chromatin decondensation.[5] Early functional studies about NETs mainly focus on their roles in immune surveillance and evidence suggests that NETs might exert dual functions during inflammation: on one hand they trap and kill microorganisms, orchestrating the resolution of neutrophil-driven inflammation,[6,7] while on the other hand, they might trap immune cells and expose them against self-antigens, exacerbating interferon-driven inflammation.[8,9] Given their versatile, context-dependent contributions to anti-microbial inflammation, role of NETs played in the pathology of other diseases has been of great clinical interest.[10]

Neutrophils constitute a major component in human hepatocellular carcinoma (HCC).[11] Prevailingly viewed as short-lived cells unless rescued by tissue-derived survival signals,[12] tumor-infiltrating neutrophils are almost entirely recruited from circulating blood.[13] Multiple evidence suggested that neutrophils represented important players in the pathophysiology of tumors.[14] For example, our recent study found that activated monocytes in peritumor stroma of human HCC could produce CXCL2 and CXCL8 to recruit and sustain the survival of neutrophils in tumor milieu, and the accumulated neutrophils could facilitate tumor metastasis through the production of oncostatin M (OSM).[15] However, functions of neutrophils are diverse and multi-layered.[16] Other functional mechanisms beyond neutrophil-produced OSM as well as mechanisms shaping the phenotypes and functions of these cells in human HCC are not yet fully uncovered. Previous studies had reported an increased release of NETs in tumor tissues, including HCC, and NETs had been implicated in promoting cancer cell migration and impacting endothelial integrity to facilitate disease progression.[17–19] However, previous studies primarily used PMA-stimulated NETs in *in vitro* experiments and the detailed mechanistic link between NETs and metastasis, especially in human HCC, had not been fully resolved. A better understanding of the presence of and precise role played by NETs in mediating

CONTACT Limin Zheng zhenglm@mail.sysu.edu.cn State Key Laboratory of Oncology in Southern China, Collaborative Innovation Center for Cancer Medicine; Yan Wu wuyan32@mail.sysu.edu.cn
*Those authors share corresponding authorship.
Supplemental data for this article can be accessed on the publisher's website

functions of neutrophils within human tumor microenvironments is an unmet need that may open novel therapeutic avenues for the disease.

Beyond cancer cells, recent studies have reported that cellular metabolic switch was involved in the regulation of immune cells under many physiological and pathological conditions.[20] But for now, little is known about whether and how metabolic changes might occur and regulate the phenotypes and functions of immune infiltrates in specific human HCC tumor microenvironments.[21] In the current study, we found that locally programmed neutrophils underwent metabolic switch in HCC tumor tissues. Up-regulation of glycolysis triggered the release of NETs through NADPH oxidase-ROS pathway in these cells, and NETs subsequently mobilized cancer cells and down-regulated levels of tight junction molecules expression on endothelial cells, thus paving the way for tumor metastasis and disease progression.

Materials and methods

Patients & specimens

Liver tissues were obtained from 144 untreated patients with pathologically confirmed HCC from the Cancer Center of Sun Yat-sen University (Guangzhou, China) or Sun Yat-sen Memorial Hospital (Guangzhou, China) between 2010 and 2020. Samples with concurrence of auto-immune disease, HIV, and syphilis were excluded. Among these patients, 80 (cohort 1) who had complete follow-up data were used for immunohistochemical and immunofluorescent analysis. Another 64 (cohort 2) were used for the isolation of neutrophils, non-tumor liver cells, and cancer cells. Non-tumor sites were defined as areas at least 3 cm away from the tumor sites. The clinical characteristics of all patients are summarized in Table S1. Blood samples were obtained from 42 healthy donors attending the Guangzhou Blood Center (Guangzhou, China). All samples were anonymously coded in accordance with local ethical guidelines (as stipulated by the Declaration of Helsinki). Written informed consent was obtained from each patient, and the study protocol was approved by the Review Board of Sun Yat-sen University Cancer Center. Heparin tubes (367884, BD Biosciences, Franklin Lakes, U.S.) were used to collect blood samples, and all blood assays were performed using fresh cells.

Animal experiments

Female C57BL/6 mice and NOD/SCID mice were purchased from GemPharmatech (Jiangsu, China) and were maintained at the Animal Experiment Center of Sun Yat-Sen University, and all procedures were approved by the Animal Care and Use Committee of Sun Yat-Sen University. Liver orthotopic hepatoma model was established as previously described.[22] In some experiments, neutrophils were purified from the peripheral blood of healthy donors and treated with or without HepG2 tumor supernatants (30%) in the presence or absence of DNase I (10 U) or GSK484 (PAD4 inhibitor, 10 μM, HY-100514, MCE, U.S.) for 12 hours. Cells were then gently washed and intravenously injected into NOD/SCID mice with established intra-hepatic HepG2 tumors every 2 days. After 14 days, mice were sacrificed. Paraffin-embedded hepatoma samples were stained with Cit-H3 antibodies, and tumor sizes and lung metastasis were measured and counted, respectively. In other experiments, DNase I (75 U per mouse), GSK484 (4 mg/kg), or DMSO were intraperitoneal injected into C57BL/6 wildtype mice with established intra-hepatic Hepa1-6 tumors daily for 14 days. Paraffin-embedded hepatoma samples were stained with Cit-H3 antibodies, and tumor sizes and lung metastasis were measured and counted, respectively.

Isolation of neutrophils from peripheral blood or tissues

Human peripheral blood samples from healthy donors were separated by ficoll density-gradient centrifugation. The pale-red granulocyte layers were collected and neutrophils were purified by removing the contaminated erythrocytes through a brief hypotonic lysis. The purity of neutrophils was determined by flow cytometry using anti-CD15 antibody. Neutrophils with >98% purity were used in subsequent experiments.

Tumor- and non-tumor-infiltrating neutrophils were obtained from paired fresh tissue samples, as described previously.[23] Briefly, Fresh HCC biopsy specimens were cut into tiny pieces and digested in RPMI 1640 supplemented with DNase I (0.05 mg/ml, DN25, Sigma-Aldrich, St. Louis, U.S.), Collagenase IV (0.05 mg/ml, C5138, Sigma-Aldrich, St. Louis, U.S.), and 20% FBS (10099–141, Gibco, NYC, U.S.) at 37°C for 40 min. Dissociated cells were separated by ficoll density-gradient centrifugation. $CD15^+$ neutrophils were isolated using magnetic beads (130–046-601, Miltenyi Biotec, Bergisch Gladbach, Germany). The purified cells were then used for direct analysis, *in vitro* or *in vivo* experiments.

To verify the purity of neutrophils from tumor and non-tumor tissues of HCC, we examined the granularity and expression of neutrophil markers for $CD15^+$ cells purified from paired tumor and nontumor liver tissues (n = 4). The results showed that most of the cells had multi-lobed shape nucleus and over 97% of these cells were $CD14^-$, $CD16^+$, $CD33^+$, and $CD66b^+$ (Figure S1A, B), confirming that these cells were predominantly neutrophils. Moreover, as shown in Figure S1C, most of the $CD14^-CD16^+CD33^+CD66b^+$ cells (99% and 98% in paired tumor and non-tumor liver tissues respectively) were $CD15^+$, excluding the possibility that a particular subset of neutrophils was preferentially enriched in the isolation process based on CD15 expression. Fluorescent-conjugated antibodies including anti-human CD14 (557923, BD Bioscience, New York City, U.S.), anti-human CD15 (48–0158, eBioscience, San Diego, U.S.), anti-human CD16 (IM0814, Beckman Coulter, Brea, U.S.), anti-human CD33 (IM2471, Beckman Coulter, Brea, U.S.), anti-human CD45 (A96416, Beckman Coulter, Brea, U.S.), and anti-human CD66b (25–0666, eBioscience, San Diego, U.S.) were used in this experiment.

Isolation and culture of HUVECs

Human umbilical vein endothelial cells (HUVECs) were isolated from umbilical vein segments as previously described.[24] HUVECs were maintained in human endothelial serum-free

medium (EC-SFM, 11111044, Life Technologies, Carlsbad, U.S.) with 20% FBS and 0.03 mg/ml endothelial cell growth supplement (02–101, Merck millipore, Billerica, U.S.).

Preparation of culture supernatants from primary cells or cell lines

HCC tumor and paired non-tumor liver biopsy specimens were digested and separated by ficoll density-gradient centrifugation as described above. The bottom layer consisting of tumor or liver cells with erythrocytes were washed and collected. The contaminated erythrocytes were removed by using an ACK Lysis Buffer (NH4CL2009, TBD Science, Tianjin, China). 10^7 non-tumor liver cells or cancer cells were suspended in 10 ml complete medium (DMEM supplemented with 10% human AB serum) and cultured in 100 mm dishes for 2 days. Supernatants (designated as N-SN and T-SN respectively) were harvested, centrifuged, and stored at −80°C before use. The specimens used for harvesting supernatants were negative for concurrent autoimmune disease, HBV, HCV, HIV, or syphilis.

Tumor cell lines (HepG2, QGY-7703, SK-Hep-1, Hela, and Hepa1-6) were purchased from American Type Culture Collection. Human normal liver cell-line HL-7702 were purchased from the Institute of Biochemistry and Cell Biology at the Chinese Academy of Science. Cells were tested for mycoplasma contamination using a single-step PCR method. Supernatants of these cell lines were prepared by plating 5×10^6 cells in 10 ml complete medium (DMEM supplemented with 10% FBS) in 100-mm dishes for 24 hours and thereafter changing the medium to DMEM supplemented with 10% human AB serum. Supernatant was collected after 48 hours and centrifuged at 450 g to remove detached cells and then centrifuged at 12,000 g to remove cell debris. The aliquots were stored at −80°C before use.

Purification of NETs

NETs were isolated from neutrophils by using a previously described method with slight modifications.[18] These cells were treated with 30% primary HCC cell culture supernatants (T-SN) or liver cell culture supernatants (N-SN) for 12 hours, and then washed and cultured for another 4 hours in complete medium (DMEM supplemented with 10% human AB serum) before their supernatants were gently aspirated and discarded. Cold PBS was used to wash and suspend the adherent NETs and neutrophils on the bottom of the wells, and then the washing solution was collected and centrifuged at 450 g to precipitate neutrophils, leaving a cell-free NETs-rich supernatant. The NETs-rich supernatant was further centrifuged at 14,000 g and re-suspended in cold PBS to a concentration corresponding to 2×10^7 neutrophils per 100 μl of PBS. The characteristics of NETs were confirmed by DNA quantifying through SYTOX green (S7020, Thermo Fisher Scientific, Waltham, U.S.) nucleic acid labeling and MPO, PR3, Cit-H3 measuring through immunoblotting.

In vitro culture of neutrophils

Neutrophils purified from the peripheral blood of healthy donors were cultured in DMEM containing 10% AB serum at a concentration of 2×10^6 cells per well. In some experiments, neutrophils were treated with 30% non-tumor liver cell supernatants (N-SN), or 30% primary HCC cancer cell supernatants (T-SN), or 30% supernatants from HepG2, QGY-7703, SK-Hep-1, Hela, or HL-7702 cell lines, in the presence or absence of glycolytic inhibitor 2DG (20 mM, D8375, Sigma-Aldrich), pentose phosphate pathway inhibitor 6AN (2 mM, A68203, Sigma-Aldrich), NOX2 inhibitor DPI (20 μM, D2926, Sigma-Aldrich), or DNase I (10 U) for indicated times. These cells were then subjected to different measurements or washed before being co-cultured with HepG2 cells or HUVECs.

In vitro co-culture of neutrophils and HepG2 cells

For HepG2 trans-endothelial invasion assay, 2×10^4 HUVECs in EC-SFM with 10% FBS were plated into the upper chamber of 24-well transwell system (8-μm pore size; Corning, NYC, U.S.) for 48 hours, until the cells reach 100% confluence. The medium was then removed and 5×10^4 CFSE (C34554, Thermo Fisher Scientific, Waltham, U.S.)-labeled HepG2 cells, which had previously been co-cultured with 1×10^5 N-SN or T-SN -pretreated neutrophils (at a 1:2 ratio) in the presence or absence of 10 U DNase I, were washed and suspended in 100 μl serum-free EC-SFM, before being added to the upper chamber, while the lower chamber was filled with 600 μl 10% FBS supplemented EC-SFM. Cells on the upper surface of the filter were wiped off after 10 hours' culture, and the CFSE-labeled HepG2 cells that have invaded though HUVEC monolayer were fixed and visualized under a Leica fluorescent microscope.

For HepG2 migration assay, HepG2 cells were co-cultured with N-SN or T-SN -pretreated neutrophils (at a 1:2 ratio) in the presence or absence of 10 U DNase I, or treated with cell-free NETs (1 μl per 100 μl culture medium) for 12 hours. 5×10^4 HepG2 cells were then washed and suspended in 100 μl serum-free DMEM before being plated into the upper chamber of 24-well transwell system (8-μm), while the lower chamber was filled with 600 μl 10% FBS supplemented DMEM. Cells were fixed and stained with crystal violet after 10 hours' culture. Cells on the upper surface of the filter were wiped off, and the migrated cells on lower surface were counted through a microscopy.

Capillary tube formation and In vitro co-culture of neutrophils and HUVECs

1×10^4 HUVECs in 50 μl serum-free EC-SFM were seeded into a Matrigel coated 96-well plate, and incubated at 37°C for 4 hours to allow capillary tube formation. Medium was then removed, and 5×10^4 N-SN or T-SN -pretreated neutrophils in the presence or absence of 10 U DNase I, or 0.5 μl isolated cell-free NETs in 50 μl serum-free EC-SFM were added to the plate. The plate was placed at 37°C and visualized for indicated times. In some experiments,

HUVECs were seeded on L-poly-lysine (AR0003, Boster, Wuhan, China) coated cover slides, before being co-cultured with N-SN or T-SN-pretreated neutrophils (at a 1:2 ratio) in the presence or absence of 10 U DNase I, or being treated with cell-free NETs (1 μl per 100 μl culture medium) for 12 hours.

Immunohistochemistry and immunofluorescence

For immunohistochemistry staining of HCC patient tissue, paraffin-embedded and formalin-fixed sections were dewaxed and blocked with hydrogen peroxide. After heat-induced antigen retrieval, the sections were incubated with anti-human CD15 (ZM-0037, ZSGB-BIO, Beijing, China) or anti-human Cit-H3 (ab5103, Abcam, Cambridge, U.K.) primary antibodies overnight at 4°C, before being stained with corresponding HRP-conjugated secondary antibodies (Dako, Copenhagen, Denmark). Sections were then visualized with diaminobenzidine (K400611, Dako, Copenhagen, Denmark) in an Envision System.

For double immunofluorescent staining of HCC patient tissue, frozen sections were fixed and blocked. The sections were incubated with anti-human CD15 and anti-human Cit-H3 primary antibodies overnight at 4°C, followed by the incubation with corresponding Alexa Fluor-conjugated secondary antibodies (Thermo Fisher Scientific, Waltham, U.S.) and 4′-6′-diamidino -2-phenylin (DAPI, D8417, Sigma-Aldrich, St. Louis, U.S.).

For multiplex immunofluorescent staining of HCC patient tissue, frozen sections were stained with anti-human GLUT1 (07–1401, Millipore, Billerica, U.S.), anti-human CD15, and anti-human Cit-H3 primary antibodies; or anti-human CD31 (ZM-0044, ZSGB-BIO, Beijing, China), anti-human CD15, anti-human Cit-H3, and anti-human VE-cad (ab33168, Abcam, Cambridge, U.K.) primary antibodies. The sections were then treated with a Tyramide Signal Amplification Kit (PPK007100100, Panovue, Beijing, China) as instructed by the manufacturer for visualization.

For immunofluorescence staining of cultured cells, neutrophils purified from HCC tumor/non-tumor liver tissues or peripheral blood of healthy donors, with or without indicated treatments, were suspended with PBS and spun onto glass slides. After being fixed, permeabilized, and blocked, these cells were stained with anti-human CD15 and anti-human Cit-H3 primary antibodies, and then incubated with corresponding Alexa Fluor-conjugated secondary antibodies and DAPI. Similarly, HUVECs growing on L-poly-lysine coated cover slides, with or without indicated treatments, were fixed, permeabilized, and blocked at room temperature. They were then incubated with anti-human VE-cad primary antibody overnight at 4°C, and subsequently incubated with Alex Fluor-conjugated secondary antibody and DAPI. All immunofluorescence staining images were visualized by ZEISS microscope (LSM780, Germany), and positive cells were quantified using ImagePro Plus software (Media Cybernetics, U.S.) and expressed as mean ± SEM in high-powered fields.

Evaluation of immunohistochemical variables

Analysis was performed by two independent observers who were blinded to the clinical outcome. At low-power field (×100), the tissue sections were screened, and the 5 most representative fields were selected using an Eclipse Ni-Uhighly versatile upright microscope combining system (Nikon Instruments, Japan). For evaluating the density of tissue-infiltrating $CD15^+$ and Cit-$H3^+$ cells, the respective areas of HCC tissues were then scanned at ×400 magnification (0.146 mm^2 per field). The number of nucleated $CD15^+$ and Cit-$H3^+$ cells at non-tumor or tumor tissues was then counted manually and expressed as cells per field.

Flow cytometry

Leukocytes were stained with fluorescent-conjugated antibodies anti-human CD15 (48–0158, eBioscience, San Diego, U.S.), anti-human GLUT1 (FAB1418A, R&D Systems, Minneapolis, U.S.), anti-human CD45 (A96416, Beckman Coulter, Brea, U.S.), or non-fluorescent-conjugated anti-human Cit-H3 antibody, and subjected to direct or indirect flow cytometry analysis. In some experiments, neutrophils were stained with CellRox (C10422, Thermo Fisher Scientific, Waltham, U.S.) to measure the intercellular ROS production. In other experiments, HUVECs were stained with annexin V and PI following the instruction of apoptosis analysis kit (BMS500FI, eBioscience, San Diego, U.S.). Data were acquired with the CytoFlex (Beckman Coulter, Brea, U.S.) and evaluated with FlowJo software version V10 (TreeStar, Ashland, U.S.).

Immunoblotting

The primary antibodies included: anti-β-actin (BM3873, Boster, Wuhan, China); anti-Cit-H3, anti-VE-cad; anti-HK2, PFKFB2, PFKFB3, GAPDH, ENO1, PGM1, PKM2, LDHA, PDK1 (Glycolysis antibody sampler kits, 8337, 12866, Cell Signaling Technology, Danvers, U.S.), HIF-1α (36169, Cell Signaling Technology, Danvers, U.S.), PR3 (ab91181, Abcam, Cambridge, U.K.), anti-p120 (PA1-39454, Life Technologies, Carlsbad, U.S.), anti-GLUT1 (07–1401, Millipore, Billerica, U.S.), anti-MPO (ZA-0197, ZSGB-BIO, Beijing, China), anti-CDH1 (3195, Cell Signaling Technology, Danvers, U.S.), anti-N-Cad (13116, Cell Signaling Technology, Danvers, U.S.), anti-Snail (3879, Cell Signaling Technology, Danvers, U.S.), and anti-Slug (9585, Cell Signaling Technology, Danvers, U.S.). HRP-conjugated goat anti-rabbit/mouse IgG antibodies were purchased from Cell Signaling Technology.

RNA isolation and reverse transcription-quantitative real-time PCR

Total RNA was extracted using Trizol reagent (15596, Life Technologies, Carlsbad, U.S.) and then used to synthesize cDNA with 5X All-In-One RT MasterMix (G492, Abm, Vancouver, Canada). The specific primers used to amplify genes are listed in Table S2. Quantitative PCR was performed according to a standard protocol using the SYBR Green Real-Time PCR MasterMix (QPK-201, TOYOBO, Osaka, Japan) in a Roche Light Cycler 480 System (Basel, Switzerland). To determine the relative fold change of different genes, their levels of expression were normalized to those of β-actin.

Measurement of MPO-DNA complex

MPO-DNA complex was measured by MPO-DNA complex ELISA Kit (MM-2467H2, MEIMIAN, Jiangsu, China) according to the manufacturer's instructions. In brief, supernatants contain MPO-DNA complex were added in microtiter plates, which were pre-coated with anti-MPO capture antibody, incubated at 37°C for 0.5 h and then washed with wash buffer. The peroxidase-labeled anti-DNA detection antibody was added and incubated at 37°C for another 0.5 h. After washed with wash buffer, the peroxidase substrate was added and incubated at 37°C for 10 mins. The optical density was measured at 450 nm using a microplate reader.

Measurement of enzyme activity

Hexokinase Colorimetric Assay Kit (HK-1-Y, Comin Biotechnology, Suzhou, China), Phosphofructokinase Activity Colorimetric Assay Kit (PFK-1-Y, Comin Biotechnology, Suzhou, China), Pyruvate Kinase Activity Assay Kit (PK-1-Y, Comin Biotechnology, Suzhou, China), Lactate Dehydrogenase Activity Assay Kit (LDH-1-Y, Comin Biotechnology, Suzhou, China), Glucose-6-phosphate Dehydrogenase Activity Assay Kit (G6PDH-1-Y, Comin Biotechnology, Suzhou, China) and NADPH oxidase Activity Assay Kit (NOX-1-Y, Comin Biotechnology, Suzhou, China) were used to measure the enzyme activity of neutrophil cells. In brief, cells were collected and washed once with PBS before being exposed to lysis buffer. The direct substrate, downstream enzymes, and substrates of downstream enzymes for the respective measured enzyme were added according to the manufacturers' descriptions. The ultimate products for each measured enzyme were NADPH or NADH, the absorbance of which could be detected at 340 nm by a spectrophotometer.

Measurement of lactate production

Lactate production in neutrophil culture supernatants were measured by Lactate Assay Kit (1200012002, Eton bioscience, San Diego, U.S.), according to the manufacturer's instructions.

Measurement of glycolytic capacity and mitochondrial respiration

Glycolytic capacity and mitochondrial respiration of neutrophils were analyzed through the XF-24 Extracellular Flux Analyzer (Agilent, Santa Clara, U.S.) as previously described.[25] Consecutive measurements of extracellular acidification rate (ECAR) and oxygen consumption rate (OCR) were obtained under basal conditions, and after the sequential addition of 10 mM glucose, 2 μM oligomycin, and 50 mM 2-DG (XF Glycolysis Stress Test Kit, Agilent, Santa Clara, U.S.); or the sequential addition of 2 μM oligomycin, 1 μM FCCP, and 0.5 μM rotenone/antimycin A (XF Cell Mito Stress Test Kit, Agilent, Santa Clara, U.S.). Samples were normalized by cell numbers before being analyzed.

Statistical analysis

Statistical tests used are indicated in the figure legends. Data were tested for normality using Shapiro–Wilk test, and variance homogeneity using Levene's test. For comparing normally distributed continuous variables, we used two-tailed Student's t test and one-way ANOVA with Bonferroni posttest for comparing two and multiple groups, respectively. For comparing variables that were not normally distributed, we used the Mann–Whitney test or Kruskall-Wallis test. Correlations between parameters were measured by Pearson correlation. The results are expressed as the means ± SEMs from at least three independent experiments. Statistical analysis was performed with GraphPad Prism 6 (GraphPad Software, La Jolla, USA), and $P < .05$ was considered statistically significant. The data generated in this study are available within the article and its supplementary data files.

Results

Elevated NETs released by tumor neutrophils predict poor survival of patients with HCC

To evaluate levels of NETs production in human tumor microenvironments, we stained paraffin-embedded serial sections of HCC samples with anti-human Cit-H3 (a NETs marker) antibody and anti-human CD15 antibody. As shown in Figure 1a, b, the formation of NETs detected by Cit-H3 expression in $CD15^+$ cells were significantly increased in tumor than those in non-tumor liver tissues (67.01 ± 10.64% for tumor and 7.82 ± 2.50% for non-tumor, n = 4). We then purified neutrophils from fresh HCC tissues and found that while tumor-derived $CD15^+$ cells markedly up-regulated levels of Cit-H3 expression in comparison to their non-tumor-derived counterparts (61.93 ± 8.53% for tumor and 14.97 ± 6.43% for non-tumor, n = 4, Figure 1c, d), some web-like DNA structures could also be observed in tumor-derived $CD15^+$ cells. Western blotting (n = 4, Figure 1e) and flow cytometry analysis (n = 13, Figure 1f, g) further confirmed the up-regulation of Cit-H3 expression by neutrophils purified from tumor tissues of patients with HCC. Consistently, levels of NETs released by tumor-purified neutrophils were significantly higher than their non-tumor-derived counterparts by evaluating their released MPO-DNA complex as previously reported (n = 3, Figure 1h),[26] while the infiltration level of total $CD15^+$ neutrophils exhibited no significant difference between tumor and non-tumor liver tissues (n = 13, Figure 1i).

To explore the potential role of NETs production in disease progression, we divided HCC patients who had received curative resection with follow-up data into two groups according to the median value of $Cit\text{-}H3^+$ cell density at non-tumor or tumor regions. While more $Cit\text{-}H3^+$ cells at tumor regions indicated worse patient survival (n = 80; $P = .012$ for overall survival [OS]; $P = .005$ for recurrence; Figure 1j), the density of $Cit\text{-}H3^+$ cells in non-tumor areas showed no correlation with either the OS or recurrence of HCC patients (n = 80; $P = .676$ for OS; $P = .887$ for recurrence; Figure 1k). Moreover, the density

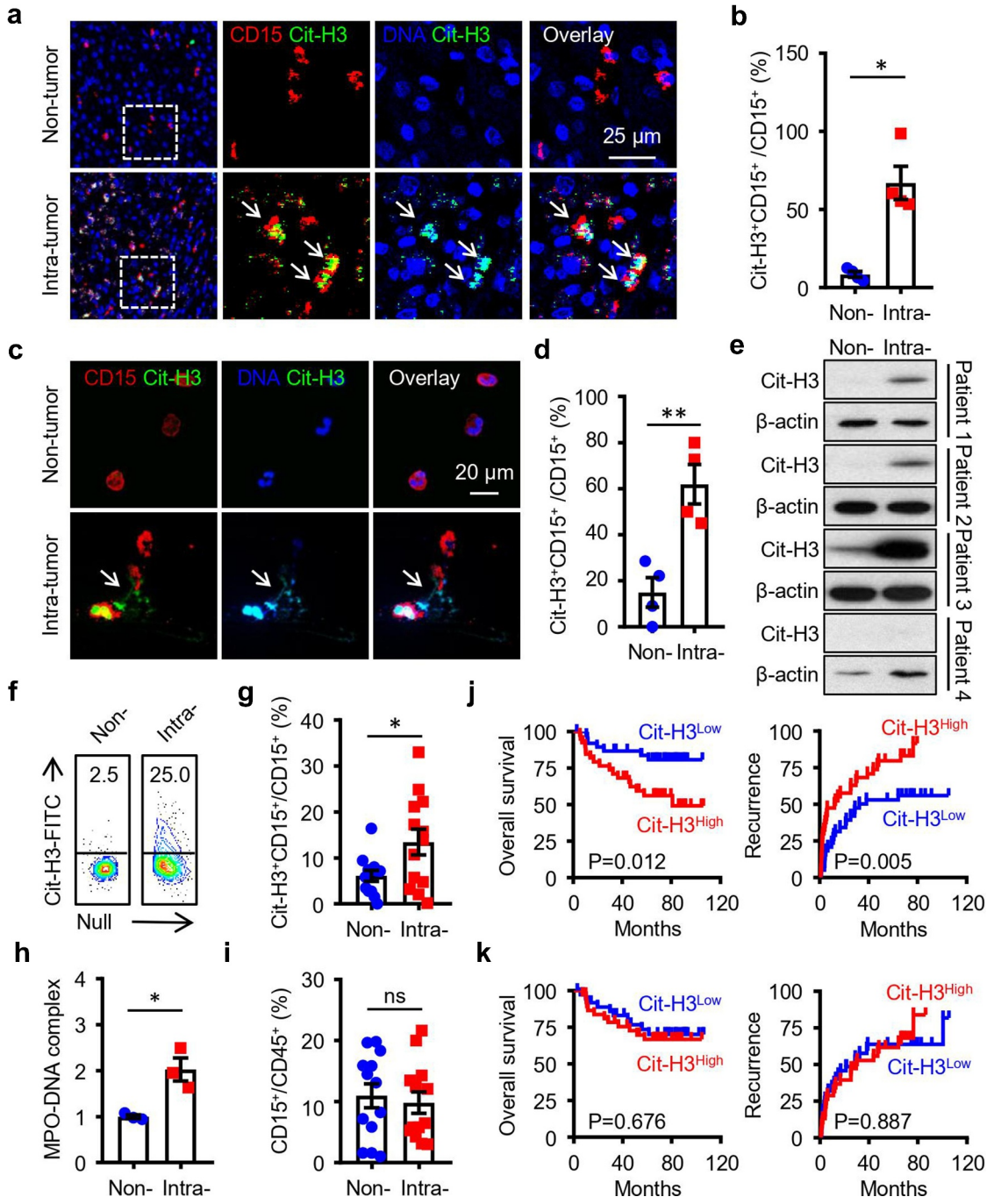

Figure 1. Elevated NETs released by tumor neutrophils predict poor survival of patients with HCC. (a, b) Paraffin-embedded HCC samples were double-stained with anti-human CD15 antibody (red) and anti-human Cit-H3 antibody (green). The distribution of $CD15^+$ $Cit\text{-}H3^+$ cells was analyzed by confocal microscopy (n = 4). Blue: DAPI. (c, d) Neutrophils were purified from paired non-tumor (Non-) and tumor tissue (Intra-) of human HCC, and seeded to cover slides before being stained with anti-human CD15 antibody (red), anti-human Cit-H3 antibody (green), and DAPI (blue). Their release of DNA and levels of Cit-H3 expression were visualized and evaluated via confocal microscopy (n = 4). (e-h) Neutrophils were purified from paired non-tumor and tumor tissue of human HCC, and their levels of Cit-H3 expression were evaluated by western blotting (**e**, n = 4; patients 1–3 have metastasis while patient 4 not) and flow cytometry analysis (f, g, n = 13). Levels of MPO-DNA complex were measured by MPO-DNA complex ELISA kit (**h**, n = 3). (i) Levels of $CD15^+$ neutrophils infiltration in paired non-tumor and tumor tissues of HCC were analyzed by flow cytometry (n = 13). (j, k) HCC patients, who received curative resection with follow-up data, were divided into two groups according to the median value of $Cit\text{-}H3^+$ cell density in tumor (j) or non-tumor (k) tissues ($Cit\text{-}H3^+$ cell: low, ≤ 8 cells per high powered field [n = 40]; high, > 8 cells per high powered field [n = 40] in tumor tissues; $Cit\text{-}H3^+$ cell: low, ≤ 1 cells per high powered field [n = 40]; high, > 1 cells per high powered field [n = 40] in non-tumor tissues). The overall survival rate (OS) and recurrence of these patients were analyzed with Kaplan–Meier method and Log-rank test. Results shown in b, d, g, h and i are expressed as the means ± SEMs. The following statistical analyses were performed: Mann–Whitney test (b), Student's *t*-test (d, g, h, i), Log-rank test (j, k). * $P < .05$, ** $P < .01$, ns, not significant.

of $Cit\text{-}H3^+$ cells at tumor tissues could serve as an independent prognostic factor for both the OS (P = .023) and recurrence (P = .004) of HCC patients (Table S3). The above results suggested that preferentially elevated NETs released by tumor infiltrating neutrophils could facilitate disease progression of human HCC.

Glycolysis is significantly enhanced in neutrophils infiltrating HCC tumor tissues

Cellular metabolism regulates and even determines the phenotypes of differently located cells,[20] so we next set out to analyze the possible relationship between metabolic switch and NETs formation in tumor neutrophils. We purified $CD15^+$ cells from non-tumor and tumor tissues of HCC patients and examined the enzyme expression levels of major metabolic pathways by Q-PCR and western blotting. As shown in Figure 2a, b, and Figure S2, $CD15^+$ cells derived from tumor tissues had increased the mRNA levels of some glycolytic enzymes, as well as the protein levels of HK2, PFKFB2, PFKFB3, GAPDH, ENO1, and PDK1 compared to $CD15^+$ cells isolated from paired non-tumor tissues. Seahorse extracellular flux analysis showed that neutrophils purified from tumor tissues exhibited significantly higher glycolytic capacity than those purified from non-tumor tissues (n = 3, Figure 2c, $p < .001$ for Figure 2d). Consistently, increased lactate production was observed in neutrophils purified from tumor tissues compared with those isolated from paired non-tumor tissues of patients with HCC (n = 3, $P = .014$, Figure 2e). Meanwhile, although tumor neutrophils also showed enhanced respiratory capacity in comparison to their non-tumor derived counterparts, the basal

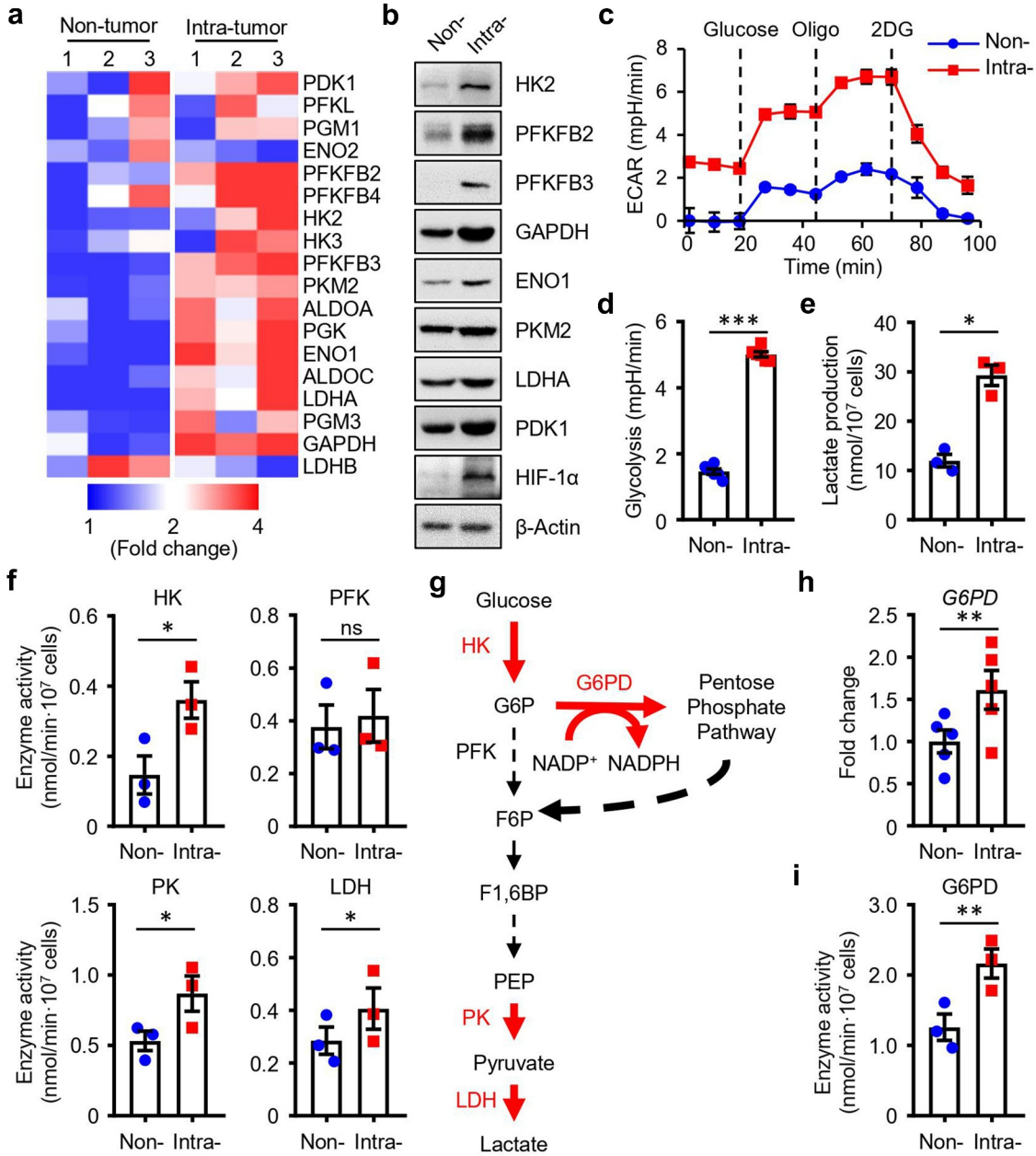

Figure 2. Glycolysis is significantly enhanced in neutrophils infiltrating HCC tumor tissues. $CD15^+$ cells were purified from paired non-tumor (Non-) and tumor tissues (Intra-) of HCC patients. (a, b) The mRNA and protein levels of key glycolysis-related enzymes in these cells were quantified by Q-PCR and western blotting, respectively (n = 3). (c, d) The extracellular acidification rate (ECAR) of these cells was measured with a seahorse analyzer (n = 3). (e) The levels of lactate production by these cells after 12 hours of *ex vivo* culture was measured with a lactate assay kit (n = 3). (f, g) The enzyme activity of HK, PFK, PK, and LDH in these cells was quantified after purification (n = 3). (h) The levels of G6PD gene expression by these cells were quantified by Q-PCR (n = 5). (i) The enzyme activity of G6PD in these cells was evaluated after purification (n = 3). Results shown in d to i are expressed as the means ± SEMs. The following statistical analyses were performed: Student's *t*-test (d, e, f, h, i), * $P < .05$, ** $P < .01$, *** $P < .001$, ns, not significant.

respiratory levels of both groups were rather low, and no significant difference in the mRNA expression levels of fatty acid oxidation enzymes (carnitine palmitoyltransferase 1A, CPT1A and medium-chain acyl-CoA dehydrogenase, MCAD) could be observed between the two groups (Figure S3A-C), suggested that there is a preferential metabolic switch in tumor-derived neutrophils.

To further map the intracellular metabolic flow of tumor neutrophils, we analyzed their glycolysis-related key enzymes activity. Interestingly, while tumor-derived neutrophils exhibited markedly higher hexokinase (HK), pyruvate kinase (PK), and lactate dehydrogenase (LDH) enzyme activity than their non-tumor derived counterparts, levels of phosphofructokinase (PFK) enzyme activity showed no significant difference between these two groups, which indicated that PFK substrate glucose-6-phosphate (G6P) might be diverted to the glycolysis branch pentose phosphate pathway (PPP), before flowing back to the downstream of glycolysis (n = 3, Figure 2f, g). To verify such hypothesis, we analyzed the mRNA expression level and enzyme activity of PPP key enzyme glucose-6-phosphate dehydrogenase (G6PD) in tumor neutrophils. As shown in Figure 2h, i, tumor-derived $CD15^+$ cells showed significantly higher levels of both mRNA expression and enzyme activity of G6PD in comparison to those isolated from paired non-tumor HCC tissues (n = 5, P = .009 for mRNA expression; n = 3, P = .004 for enzyme activity). Since PPP pathway had been implicated to be involved in the regulation of NETs release in PMA-stimulated neutrophils,[27] the above data together suggested that the preferential elevated glycolysis in tumor infiltrating neutrophils might contribute to their increased release of NETs in tumor milieus via the enhancement of PPP.

Glycolytic activation mediates the release of NETs by tumor neutrophils

To confirm the relationship between Glycolysis, PPP, and NETs, we purified $CD15^+$ cells from paired non-tumor and tumor tissues of HCC. As shown in Figure 3a, patients with increased levels of Cit-H3 expression in tumor-derived neutrophils also displayed higher levels of glucose transporter glucose transporter 1 (GLUT1) expression in those cells, compared to their non-tumor-isolated counterparts (n = 3). Flow cytometry analysis showed that when tumor neutrophils were divided into two groups according to their levels of GLUT1 expression, the $GLUT1^+$, rather than the $GLUT1^-$ cells exhibited high levels of Cit-H3 expression (n = 6; P = .002. Figure 3b, c). Consistently, levels of GLUT1 expression were found positively correlated with those of Cit-H3 in tumor-derived neutrophils (n = 14; R = 0.756; P = .002. Figure 3d). *In situ* staining of paraffin-embedded HCC samples with anti-human CD15, anti-human Cit-H3, and anti-human GLUT1 antibodies confirmed that $CD15^+$ neutrophils positive for GLUT1 expression were also positive for Cit-H3 staining in tumor tissues (n = 3. Figure 3e).

We went on to establish an *in vitro* model to verify the possible regulatory effects of glycolysis on NETs production. Neutrophils purified from peripheral blood of healthy donors were treated with supernatants from primary HCC cancer cells (T-SN) or paired non-tumor liver cells (N-SN) for 12 hours, before subjected to western blotting, enzyme activity/lactate production tests, as well as confocal analysis. Results showed that T-SN-exposed neutrophils exhibited similar phenotypes to their tumor tissue-derived counterparts, including up-regulated enzyme activities of glycolytic/PPP key enzymes with the exception of PFK, and increased levels of lactate production (Figure S4), enhanced Cit-H3 expression, presence of web-like NETs structures, and increased release of NETs in comparison to N-SN-exposed control neutrophils (Figure S5A-C). Moreover, supernatants from different types of tumor cell lines (but not supernatants from normal liver cell-line HL-7702) could similarly induced the up-regulation of Cit-H3 expression in healthy neutrophils (Figure S5D, E), indicating that tumor-induced NETs release might not be restricted to HCC-associated neutrophils.

When neutrophils isolated from peripheral blood of healthy donors were treated with glycolysis inhibitor 2-deoxy-D-glucose (2DG) or PPP key enzyme G6PD inhibitor 6-aminonicotinamide (6AN) before exposure to T-SN, their tumor-induced Cit-H3 up-regulation and DNA release were significantly antagonized compared to the T-SN alone treatment groups (n = 3. Figure 3f, g). These data confirmed that glycolysis and PPP activation were involved in the regulation of NETs release by tumor-treated neutrophils.

Glycolytic activation induced the release of NETs via NOX-ROS pathway

The production of reactive oxygen species (ROS), which generate mainly from the cytosolic NADPH oxidase (NOX) in neutrophils, is necessary for NETs formation.[28] As a main source of nicotinamide adenine dinucleotide phosphate (NADPH), PPP had been suggested to fuel NOX with NADPH to produce ROS. As expected, NOX activity and ROS production were up-regulated in T-SN (primary HCC cancer cell supernatants)-exposed healthy neutrophils compared with those in N-SN (paired non-tumor liver cell supernatants)-treated control cells, and notably, such tumor-induced ROS up-regulation could be efficiently antagonized by the treatment of neutrophils with either glycolysis inhibitor 2DG or G6PD inhibitor 6AN (n = 3, Figure 4a; n = 7, Figure 4b, c). Moreover, when healthy peripheral blood-derived neutrophils were pre-treated with NOX inhibitor diphenyleneiodonium chloride (DPI) before exposure to T-SN, their levels of ROS production, as well as Cit-H3 expression were significantly attenuated compared with the T-SN alone treatment group (n = 6; Figure 4d-f).

To further confirm the regulatory role of NOX-ROS in mediating tumor-induced Cit-H3 up-regulation in clinical samples, neutrophils were purified from tumor tissues of patients with HCC, and examined for their levels of GLUT1, ROS, and Cit-H3 expression through flow cytometry analysis. As shown in Figure 4g, h, levels of ROS production were positively correlated with those of GLUT1 expression (n = 12; R = 0.752; P = .005) and Cit-H3 expression (n = 12; R = 0.761; P = .007) in tumor-derived neutrophils. The above results

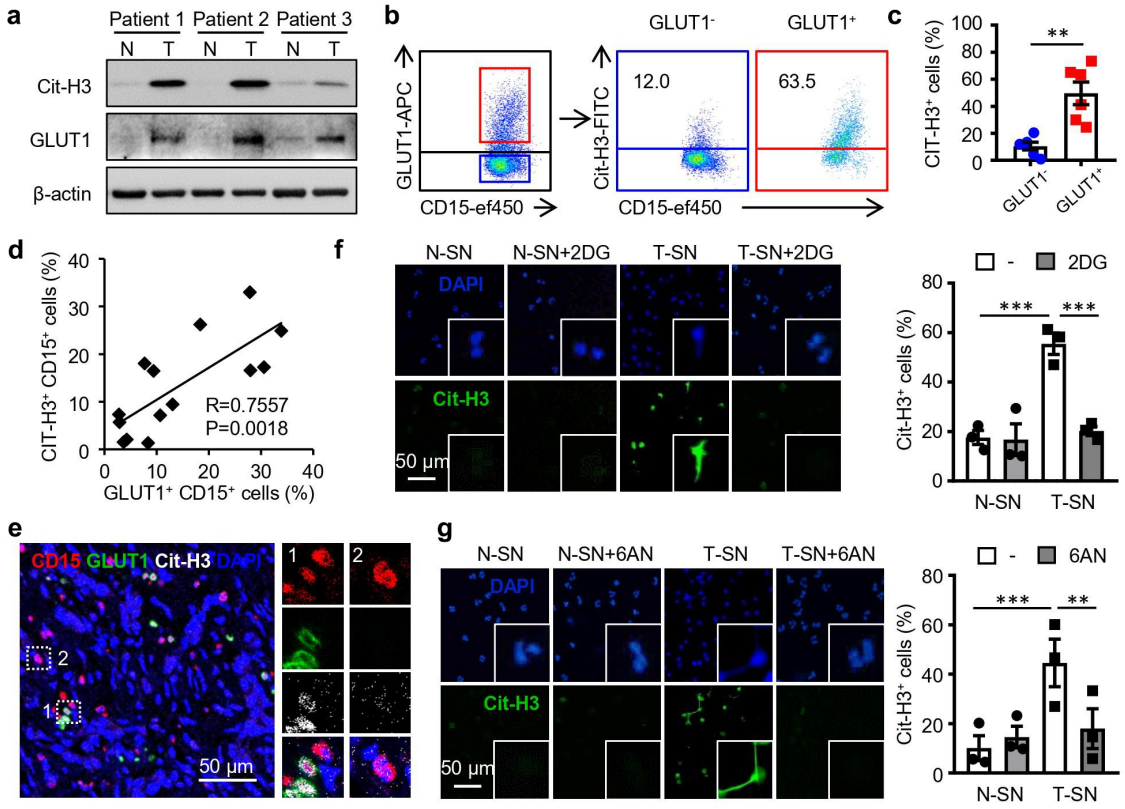

Figure 3. Glycolytic activation mediates the release of NETs by tumor neutrophils. (a) CD15$^+$ cells were purified from paired non-tumor and tumor tissues of HCC patients, and their levels of Cit-H3 and GLUT1 expression were quantified by western blotting (n = 3). (b-d) CD15$^+$ cells were purified from tumor tissues of HCC patients. The levels of and correlations between Cit-H3 and GLUT1 expression in these cells were analyzed by flow cytometry (n = 6 in b, c; n = 14 in d). (e) Paraffin-embedded HCC samples were stained with anti-human CD15 antibody (red), anti-human Cit-H3 antibody (white), anti-human GLUT1 antibody (green), and DAPI (blue). The co-expression of Cit-H3 and GLUT1 on CD15$^+$ tumor-infiltrating neutrophils was analyzed by confocal microscopy (n = 3). (f, g) CD15$^+$ cells were purified from peripheral blood of healthy donors and treated with 30% primary HCC cancer cell supernatants (T-SN) or paired non-tumor liver cell supernatants (N-SN) for 12 hours, in the presence or absence of glycolytic inhibitor 2DG or G6PD inhibitor 6AN. These cells were then stained with anti-human Cit-H3 antibody (green), and their release of DNA and levels of Cit-H3 expression were visualized and evaluated by confocal microscopy (n = 3). Blue: DAPI. Results shown in c, f, and g are expressed as the means ± SEMs. The following statistical analyses were performed: Student's t-test (c), Pearson correlation and linear regression analysis (d), one-way ANOVA with Bonferroni posttest (f, g). * $P < .05$, ** $P < .01$, *** $P < .001$.

suggested that NOX-ROS pathway was involved in mediating the NETs-inducing effects of glycolytic activation in HCC tumor associated neutrophils.

NETs up-regulate the migratory ability of cancer cells

While neutrophils are prone to apoptosis under normal physiological conditions,[12] our recent study found that these cells were recruited, survived, and accumulated in HCC tumor tissues in response to tumor environmental cues.[15,23,29] Of note, analysis of patient' clinicopathological characteristic data showed that the density of Cit-H3$^+$ cells in tumor tissues, calculated through IHC staining of paraffin-embedded samples with anti-human Cit-H3 antibody, was positively associated with the metastasis potential of HCC patients (n = 80; $P = .001$. Table S4), indicating that the better survived neutrophils might facilitate tumor metastasis via the release of NETs in human HCC.

To confirm the above hypothesis, we treated healthy peripheral neutrophils with N-SN or T-SN, in the presence or absence of DNase I for 12 hours. As shown in Figure 5a, b, DNase I could effectively destruct NETs extension released by T-SN-exposed neutrophils, while not impacting cell viability (Figure S6), thus representing an effective way to evaluate the "loss of function" effects of NETs. *In vitro* HepG2 cancer cell trans-endothelial migration assays were then performed, and the results showed that while T-SN-treated neutrophils could significantly up-regulated the trans-endothelial migration of HepG2 cells compared to the N-SN-exposed neutrophils, such effects could be efficiently antagonized by the treatment of neutrophils with DNase I (n = 4. Figure 5c, d).

Consistently, DNase I could attenuate the T-SN-treated-neutrophil-induced up-regulation of cancer cells transmembrane migration ability compared to control groups (Figure 5e), and NETs purified from the culture supernatants of T-SN-pretreated neutrophils, as confirmed to be high in PR3, MPO, and Cit-H3 expression compared to those derived from N-SN-exposed neutrophils (Figure 5f), could mimic the effects of tumor neutrophil cells by driving the significant transmembrane migration of cancer cells (Figure 5g, h). Moreover, NETs purified from T-SN-pretreated neutrophils could induced decreased cadherin 1 (CDH1) expression and increased N-Cadherin (N-Cad), Snail, Slug expression in HepG2 cells compared to their N-SN-exposed neutrophils-derived counterparts (Figure S7). Together, these data suggested that tumor neutrophils might facilitate HepG2 cancer cells epithelial–mesenchymal transition (EMT) and migration through the release of NETs.

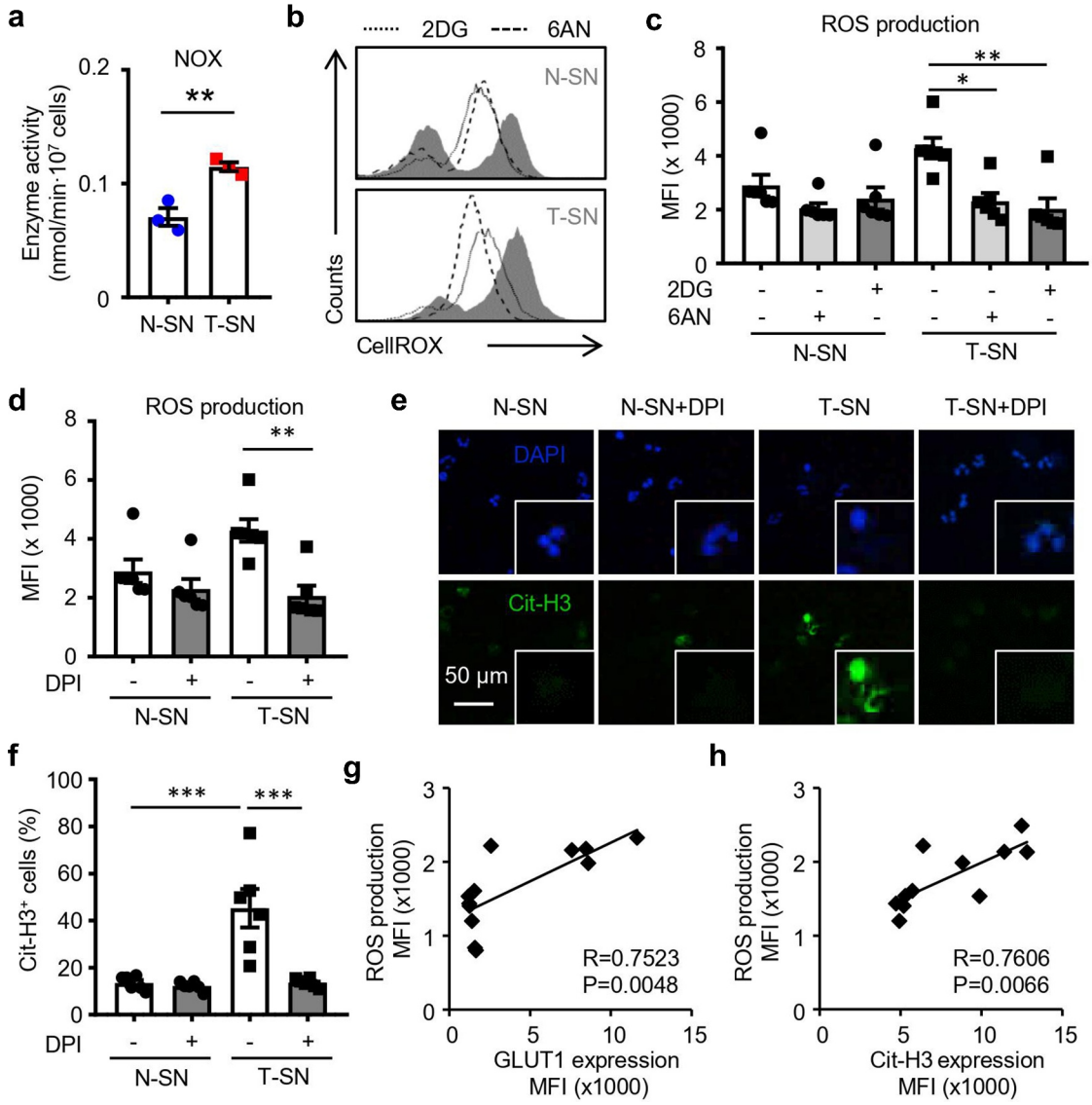

Figure 4. Glycolytic activation induced the release of NETs via NOX-ROS pathway. CD15$^+$ cells were purified from peripheral blood of healthy donors and treated with 30% primary HCC cancer cell supernatants (T-SN) or paired non-tumor liver cell supernatants (N-SN) for 12 hours, in the presence or absence of 2DG, or 6AN, or DPI. (a) The enzyme activity of NOX in these cells was quantified (n = 3). (b-d) Levels of ROS production by these cells were evaluated by flow cytometry (n = 6). (e, f) Levels of Cit-H3 expression in these cells were analyzed by confocal microscopy (n = 6). Green: Cit-H3; Blue: DAPI. (g, h) CD15$^+$ cells were purified from tumor tissues of HCC patients. Correlations between levels of ROS, GLUT1, and Cit-H3 expression in these cells were determined by flow cytometry (n = 12). Results shown in a, c, d, and f are expressed as the means ± SEMs. The following statistical analyses were performed: Student's t-test (**a**), Kruskal–Wallis test followed by Dunn's posttest (c, d), one-way ANOVA with Bonferroni posttest (f), Pearson correlation and linear regression analysis (g, h). * $P < .05$, ** $P < .01$, *** $P < .001$.

NETs induce the down-regulation of VE-cadherin on endothelial cells and correlate with tumor vasculature integrity

Tumor metastasis reflects on one hand the mobility of cancer cell itself, and on another hand the integrity of vascular structure.[30] In light of the above results concerning effects of NETs on cancer cell mobility, we wondered whether NETs also influenced the integrity of vascular structures. To that end, we established an *in vitro* human umbilical vein endothelial cell (HUVEC) co-culture system, in which neutrophils were purified from the peripheral blood of healthy donors and pre-treated with N-SN or T-SN, before co-cultured with the HUVEC cells. As shown in Figure S8A, B, T-SN-exposed neutrophils significantly reduced the number of branch points and length of vasculature-like tubes formed by HUVEC cells compared to the N-SN-treated neutrophils, and such effects could be rescued by pre-treating the T-SN-exposed neutrophils with DNase I. Accordingly, NETs purified from the culture supernatants of T-SN-pretreated neutrophils could mimic the effects of their originating cells by similarly disrupting the integrity of HUVEC-formed structures (n = 4). Interestingly, tumor-treated neutrophils did not up-regulate the apoptosis of HUVEC cells (n = 6. Figure S8C), indicating that NETs released by tumor neutrophils might induce the partial breakdown of vasculature via non-apoptosis-dependent pathways.

We went on to investigate mechanisms mediating the effects of NETs on endothelial cells by isolating NETs from N-SN or T-SN -pre-treated neutrophils. As shown in Figure 6a, NETs from T-SN-exposed neutrophils significantly down-regulated the expression levels of key adhesion molecules VE-cadherin (VE-cad) and catenin δ-1 (p120) in HUVEC cells, compared with those isolated

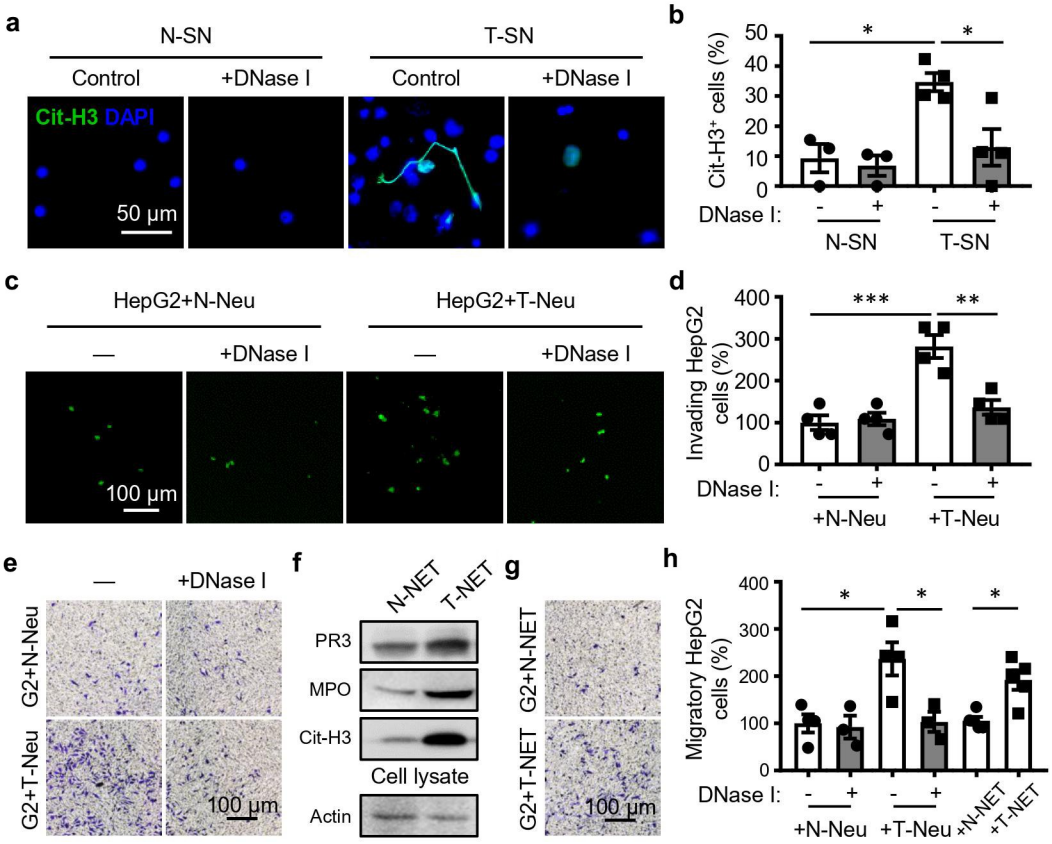

Figure 5. NETs up-regulate the migratory ability of cancer cells. $CD15^+$ neutrophils were purified from peripheral blood of healthy donors. (a, b) $CD15^+$ neutrophils were treated with 30% primary HCC cancer cell supernatants (T-SN) or paired non-tumor liver cell supernatants (N-SN) for 12 hours, in the presence or absence of DNase I, before being stained with anti-human Cit-H3 antibody. Their release of DNA (blue) and levels of Cit-H3 expression (green) in total $CD15^+$ cells were visualized and evaluated by confocal microscopy (n = 3 to 4). (c, d) CFSE-stained HepG2 cells were added to the upper chamber of an endothelial-cell-pre-seeded transwell system, with the combination of N-SN-pretreated neutrophils (N-Neu) or T-SN-pretreated neutrophils (T-Neu), in the presence or absence of DNase I. The trans-endothelial migration of HepG2 cells were calculated after 10 hours culture (n = 4). The data of "HepG2 + N-Neu" group was normalized to 100%. (e) HepG2 cells were cultured with N-Neu or T-Neu in the presence or absence of DNase I for 12 hours before being washed and seeded into the upper chamber of a transwell system. The transmembrane migration ability of HepG2 cells were calculated after 10 hours culture (n = 4). (f) $CD15^+$ cells were pre-treated with 30% N-SN, or T-SN for 12 hours. These cells were then washed and cultured for another 4 hours before their NETs were harvested (designated as N-NET or T-NET, respectively). Levels of PR3, MPO and Cit-H3 expression in NETs were analyzed by western blotting (n = 3). (g) HepG2 cancer cells were pre-treated with N-NET or T-NET for 12 hours before being seeded into the upper chamber of a transwell system. The transmembrane migration ability of HepG2 cancer cells were calculated after 10 hours' culture (n = 5). (h) Statistics of e and g were shown, and data of the "HepG2 + N-Neu" group was normalized to 100%. Results shown in b, d, and h are expressed as the means ± SEMs. The following statistical analyses were performed: one-way ANOVA with Bonferroni posttest (b, d, h), Student's *t*-test (comparison between N-NET and T-NET groups in **h**). * $P < .05$, ** $P < .01$, *** $P < .001$.

from N-SN pre-treated neutrophils. The decrease of VE-cad expression on NETs-treated HUVECs was also confirmed through confocal analysis (n = 5. Figure 6b, c). Consistently, while T-SN-treated neutrophils down-regulated levels of VE-cad expression on HUVEC cells compared with N-SN-exposed neutrophils, such effects could be efficiently antagonized by treating the neutrophils with DNase I (n = 5. Figure 6d-f).

To verify the role of NETs on vasculature integrity in tumors *in situ*, we stained paraffin-embedded serial section of HCC samples with anti-human CD31 antibody, anti-human Cit-H3 antibody, and anti-human VE-cad antibody. As shown in Figure 6g, some $CD31^+$ cells showed low expression of VE-cad, where Cit-$H3^+$ cells were in close proximity, while other $CD31^+$ cells exhibited relatively high levels of VE-cad expression where Cit-$H3^+$ cells were absent (n = 3). To quantify these visual data, micrograph of each patient was divided into 100 μm×100 μm grids. Eight grids with positive VE-cad expression on $CD31^+$ cells (VE-cad^+) and eight grids with negative VE-cad expression on $CD31^+$ cells (VE-cad^-) were randomly selected, and the infiltration levels of Cit-$H3^+$ cells in these grids were calculated. As shown in Figure 6h, the VE-cad^+ group showed significantly lower levels of Cit-$H3^+$ cells present in proximity than their VE-cad^- counterparts (n = 3). These data suggested that in addition to increasing cancer cell mobility, NETs might also disrupt the vasculature integrity in tumor tissues by down-regulating the expression level of adhesion molecule VE-cad on endothelial cells, which, together, contribute to the facilitation of tumor intravasation.

NETs depletion inhibits tumor metastasis in mice in vivo

We further evaluated the effects of NETs on tumor growth in mice *in vivo*. Neutrophils were purified from the peripheral blood of healthy donors and treated with or without HepG2 human cell-line supernatants in the

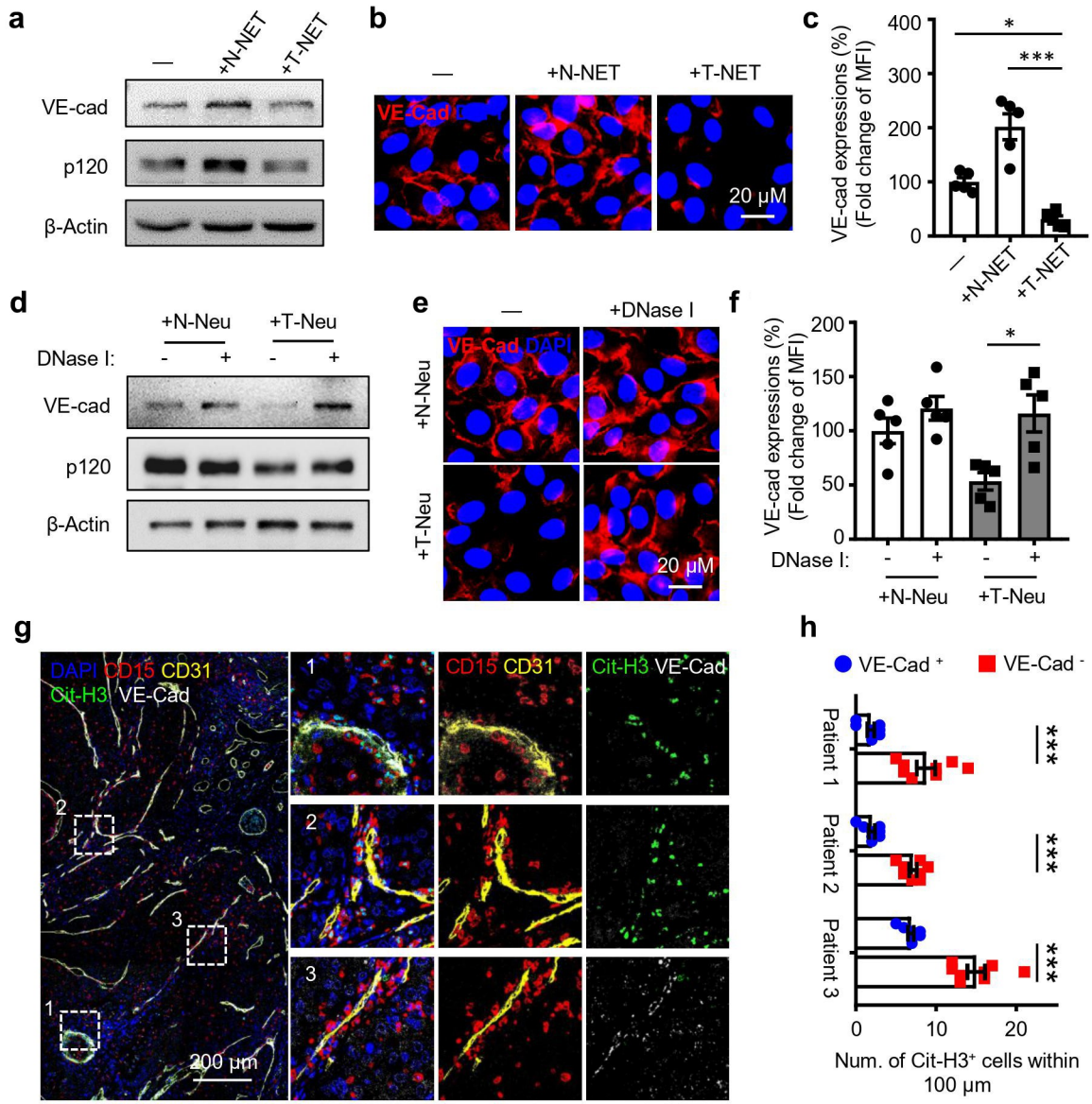

Figure 6. NETs induce the down-regulation of VE-cadherin on endothelial cells and correlate with tumor vasculature integrity. (a-c) $CD15^+$ neutrophils were purified from peripheral blood of healthy donors. These cells were pre-treated with 30% non-tumor liver cell supernatants (N-SN) or primary HCC cancer cell supernatants (T-SN) for 12 hours, and then washed and cultured for another 4 hours to harvested NET (N-NET or T-NET, respectively). HUVEC cells were left untreated or treated with N-NET or T-NET for 12 hours. Their levels of p120 expression were quantified by western blotting. Levels of VE-cad expression in HUVEC were analyzed by both western blotting (a) and confocal microscopy (b) (n = 5). Red: VE-cad; Blue: DAPI. (d-f) $CD15^+$ neutrophils were purified from peripheral blood of healthy donors and treated with 30% N-SN or T-SN for 12 hours (designated as N-Neu and T-Neu respectively) before being washed and co-cultured with HUVEC cells, in the presence or absence of DNase I. The wells were washed after 12 hours' co-culture to remove neutrophils, and levels of p120 expression in HUVEC cells were quantified by western blotting. Levels of VE-cad expression in HUVEC cells were analyzed by both western blotting (d) and confocal microscopy (e) (n = 5). Red: VE-cad; Blue: DAPI. (g, h) Paraffin-embedded HCC samples were stained with anti-human CD31 antibody (yellow), anti-human CD15 antibody (red), anti-human Cit-H3 antibody (green), anti-human VE-cad antibody (white), and DAPI (blue). The distribution of different signals was determined by confocal microscopy (g). The micrograph of each patient was divided into 100 μm×100 μm grids. 8 grids with positive VE-cad expression on $CD31^+$ cells ($VE\text{-}cad^+$) and 8 grids with negative VE-cad expression on $CD31^+$ cells ($VE\text{-}cad^-$) were randomly selected, and the infiltration levels of $Cit\text{-}H3^+$ cells in these grids were calculated (h). (n = 3). Results shown in c, f, and h are expressed as the means ± SEMs. The following statistical analyses were performed: one-way ANOVA with Bonferroni posttest (c, f), Student's *t*-test (**h**). * $P < .05$, *** $P < .001$.

presence or absence of DNase I or GSK484 (PAD4 inhibitor). Cells were then gently washed and intravenously injected into NOD/SCID mice with established intra-hepatic HepG2 tumors. As shown in Figure 7a-c, neutrophils pre-treated with tumor supernatants significantly increased their release of NETs ($Cit\text{-}H3^+$ signals) in tumor *in situ*, and induced more tumor lung metastasis *in vivo* compared to normal neutrophils control. Both DNase I and PAD4 could antagonize the up-regulation of $Cit\text{-}H3^+$ signals in tumor-exposed-neutrophils treatment group *in situ*, and markedly abrogate neutrophil-induced tumor metastasis *in vivo* significantly. In contrast, tumor-exposed neutrophils did not impact tumor growth *in situ* (Figure 7d). Moreover, when DNase I and GSK484 were intraperitoneal injected into C57BL/6 wildtype mice with established intra-hepatic Hepa1-6 tumors, they did not affect tumor growth *in vivo*, but could both reduce the infiltration of $Cit\text{-}H3^+$ cells in tumor tissues and

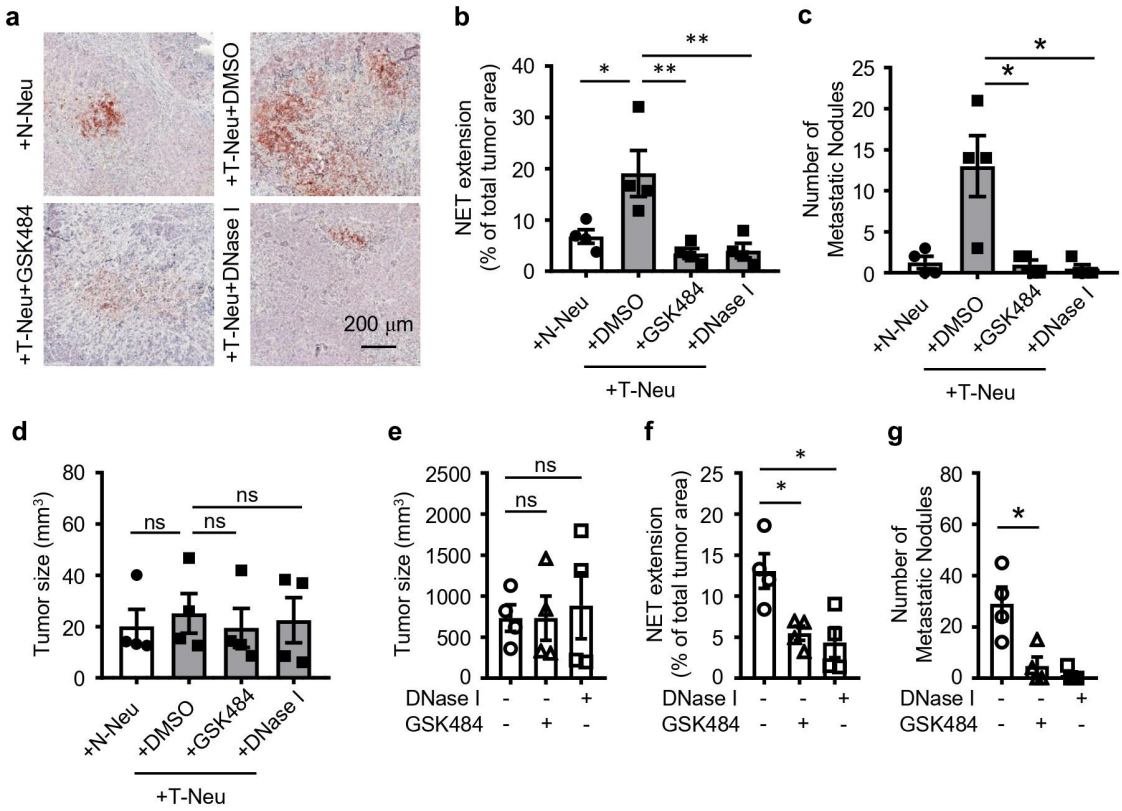

Figure 7. NETs depletion inhibits tumor growth in mice in vivo. (a-d) Neutrophils purified from the peripheral blood of healthy donors were treated with or without HepG2 tumor supernatants (30%) in the presence or absence of DNase I or GSK484 (PAD4 inhibitor) for 12 hours. Cells were then gently washed and intravenously injected into NOD/SCID mice with established intra-hepatic HepG2 tumors every 2 days. After 14 days, mice were sacrificed. (a, b) Paraffin-embedded hepatoma samples were stained with Cit-H3 antibodies, and tumor sizes (d) and lung metastasis (c) were measured and counted respectively. (e-g) DNase I, GSK484, or DMSO were intraperitoneal injected into C57BL/6 wildtype mice with established intra-hepatic Hepa1-6 tumors daily for 14 days. (f) Paraffin-embedded hepatoma samples were stained with Cit-H3 antibodies, and tumor sizes (e) and lung metastasis (g) were measured and counted respectively. There were 4 representatives for each group in a-g. Results shown in b to g were expressed as the means ± SEMs. The following statistical analyses were performed: one-way ANOVA with Bonferroni posttest (b, e, f), Kruskal–Wallis test followed by Dunn's posttest (c, d, g). * $P < .05$, ** $P < .01$, ns, not significant.

prohibit lung tumor metastasis compared to control groups (Figure 7e-g). These data indicated that NETs could facilitate tumor metastasis in mice *in vivo*.

Discussion

Neutrophils are known to function as first responders specialized in pathogen clearance and as prototypic effector cells of inflammatory responses.[16] Their release of NETs has been reported to play key roles in regulating these processes according to various experimental models.[10] Neutrophils also constitute major components in human HCC and the current study found that they were of high metabolic plasticity in specific tumor regions. Locally instructed by tumor microenvironments, neutrophils up-regulated levels of glycolysis and PPP, which induced the release of NETs. NETs then subsequently mobilized cancer cells and disrupted vascular integrity, thus facilitating tumor metastasis of human HCC.

Within highly stressful microenvironments, cancer cells could delicately tilt their metabolic flow to adapt to, and make the best of what they are surrounded by.[31] Notably, recent studies showed that stromal cells also tend to exhibit metabolic switch that might result in facilitated tumor progression.[21] Compared with other major tissue components, such as macrophages and T lymphocytes, the metabolic status and its clinical significance of tumor associated neutrophils, were much less documented, especially in human neoplasms. The present study found that levels of glycolysis were significantly up-regulated in neutrophils from tumor than paired non-tumor tissue, which might be mediated by the increased stabilized HIF-1α in these cells, and the glycolytic activities were positively correlated with NETs release by neutrophils in tumor regions of human HCC. Interesting, glycolysis was not proportionately increased throughout its pathway. It seemed, instead, to be tilted to the PPP branch before flowing back to the mainstream pathway. Inhibition of glycolysis and PPP could both lead to the attenuated release of NETs. Consistently, tissue sample *in situ* analysis confirmed that most neutrophils expressing up-regulated GLUT1 were also positive for Cit-H3 staining. We also noticed that levels of oxidative phosphorylation (OXPHOS) were higher in tumor neutrophils than those derived from non-tumor tissues, but the basal levels of OXPHOS from both groups were rather low, which might due to the relatively few mitochondria present in neutrophils as previously reported.[32]

There are two important outcomes of the PPP pathway – namely, nucleotide production (which happens during cell proliferation) and NADPH production,[33] which could fuel NOX to produce ROS. Our study provided several lines of

evidence to support the role of NOX-ROS in mediating NETs release induced by neutrophil glycolysis-PPP activation in human HCC. First, levels of both NOX enzyme activity and ROS were significantly up-regulated in tumor treated neutrophils compared with normal control. Second, the up-regulation of ROS in tumor neutrophils could be efficiently antagonized by the treatment of these cells with either glycolysis inhibitor 2DG or G6PD inhibitor 6AN. Third, NOX inhibitor DPI could attenuate the tumor-induced ROS, as well as Cit-H3 up-regulation in neutrophils. Consistently, levels of ROS production were found positively correlated with those of GLUT1 expression and Cit-H3 expression in neutrophils derived from HCC tumor tissues.

Previous study had found increased NET release in HCC patients, particularly those with metastatic cancer,[17] but such study primarily used LPS or PMA-stimulated NETs in *in vivo* or *in vitro* experiments and the detailed mechanistic link between NETs and metastasis had not been fully resolved. It has been acknowledged that tumor intravasation requires the enhanced motility of cancer cells and the loose connection between endothelial cells.[30] Our current study provided evidence that NETs released by tumor infiltrating neutrophils facilitated both processes by up-regulating the migration ability of cancer cells and at the same time down-regulating VE-cad expression on endothelial cells. It should be noted that the vasculature system in tumor tissues might be dynamically modulated by regional environmental cues.[34] Our previous study showed that in peritumor stroma of human HCC, activated monocytes could induce IL17A-producing T cell expansion and subsequent neutrophil recruitment, which then facilitated tumor angiogenesis by the release of matrix metalloproteinase-9 (MMP9).[29,35] Our current results complemented such findings by showing that in tumor regions with established vasculature, neutrophils might reduce the tight junction between endothelial cells and disrupt vascular integrity at such a degree as to facilitate tumor intravasation by the release of NETs. The distinct effects on vasculature system exerted by tumor associated neutrophils might reflect, on one hand, the specific phenotypes/functions of these cells in response to different local environmental signals, and on another hand, the specific needs of different vascular developmental stage of a same tumor.

We also noticed that most NETs-producing neutrophils were present in close proximity to vessels in HCC tumor tissues. The distinct pattern of distribution of neutrophils might be rationalized as to not only temperately release these cells from the grip of general glucose-deprivation in tumor microenvironments and enable their up-regulation of glycolysis, but also facilitate the pro-intravasation functions of NETs released by these cells. Accordingly, clinical data analysis confirmed that most $CD31^+$ cells showed low expression of VE-cad, where Cit-$H3^+$ cells were in close proximity, and that levels of Cit-$H3^+$ cells infiltration were inversely correlated with those of VE-cad expression on $CD31^+$ cells in tumor tissues, while positively correlated with the metastasis potential of human HCC. These data also complement our recent finding that monocytes-recruited neutrophils promoted tumor metastasis via producing OSM by showing that where these cells were close to vessels,[15] they could undergo further metabolic switch to facilitate regional metastasis through the releasing of NETs.

Our and other groups' previous studies have showed that tumor-derived soluble factors, such as cytokines, hyaluronan fragments, and metabolites could play roles in regulating the phenotypes and functions of tumor-associated neutrophils.[23,36] But, whether these or what other components might be involved in triggering the metabolic switch and subsequent NETs release in the current model were still undetermined and required further examination. Moreover, NETs can exert their functions via molecules attached on the released DNA scaffold or the DNA scaffold itself. The use of DNase I in the present study could not clarify which mechanism might be involved in regulating cancer cell mobility and VE-cad expression on endothelial cells by NETs, nor could it define whether the same or different mechanisms were involved with regard to cancer cells and endothelial cells. Further study would be needed to address these questions. In addition, mechanisms involved in NET-induced VE-cad down-regulation on endothelial cells also required further exploration.

Nonetheless, the current study unveiled a novel mechanism by which locally instructed neutrophils metabolically shifted to glycolysis-PPP pathway, which subsequently induced the production and release of NETs and facilitated tumor metastasis of human HCC. Given the role of glycolysis in regulating NETs release by tumor-associated neutrophils, it is tempting to assume that a glycolytic inhibitor would improve the efficacies of current therapeutics targeting tumor metastasis, especially for patients with high levels of tissue-infiltrating neutrophils. In addition, inhibitors that antagonize glycolytic activation might target not only the NETs-releasing neutrophils but also cancer cells with high glycolytic rates in tumor microenvironments, thus representing an attractive therapeutic treatment with possible dual targets. Together, the present study provided a novel tumor immune editing strategy and indicated efficient targets for future immune-based anti-cancer therapies.

Abbreviations2DG, 2-deoxy-D-glucose; 6AN, 6-aminonicotinamide; Cit-H3, citrullinated histone H3; CPT1A, carnitine palmitoyltransferase 1A; DPI, diphenyleneiodonium chloride; ECAR, extracellular acidification rate; EMT, epithelial–mesenchymal transition; G6P, glucose-6-phosphate; G6PD, glucose 6-phosphatedehydrogenase; HCC, hepatocellular carcinoma; HK, hexokinase; HUVEC, human umbilical vein endothelial cell; LDH, lactate dehydrogenase; LPS, lipopolysaccharide; MCAD, medium-chain acyl-CoA dehydrogenase; MMP9, matrix metalloproteinase-9; MPO, myeloperoxidase; NADPH, nicotinamide adenine dinucleotide phosphate; NE, neutrophil elastase; NET, neutrophil-extracellular trap; NOX, NADPH oxidase; N-SN, liver cell culture supernatant; OCR, oxygen consumption rate; PAD4, protein arginine deiminase 4; PFK, phosphofructokinase; PK, pyruvate kinase; PMA, phorbol-12-myristate-13-acetate; PPP, pentose phosphate pathway; PR3, proteinase 3; ROS, reactive oxygen species; T-SN, primary HCC cell culture supernatant; TSN, tumor culture supernatant.

Acknowledgments

We thank Prof. Chao Liu and Dr. Chao-qun Liu from the Sun Yat-sen Memorial Hospital, for providing the HCC tissue specimen and related clinical information.

Authors' contributions

Z.Z.J. designed the experiments, performed flow cytometry, processed tissues and western blotting, collected the data, and wrote the paper. Z. P.P., X.C.L., and H.F.G. helped and performed seahorse experiments, enzyme activity and lactate production detections. M.M.Z., W.R.N., D.J., and Y.F.H did immunohistochemical staining and analyzed the data. L. Z. and Y.W. advised and consulted on analyzing human data, planned and supported the project, analyzed data, and wrote the paper. All authors read and approved the final manuscript.

Disclosure statement

The authors declare no competing financial interests.

Funding

This work was supported by the Guangdong Science and Technology Department [2020B1212060031]; National Natural Science Foundation of China [82071743]; National Natural Science Foundation of China [81730044]; National Natural Science Foundation of China [91842308]; National Key R&D Program of China [2021YFC2300601]; Guangdong Basic and Applied Basic Research Foundation [2020A1515111000]; National Key R&D Program of China [2017YFA0505803].

References

1. Brinkmann V, Reichard U, Goosmann C, Fauler B, Uhlemann Y, Weiss DS, Weinrauch Y, Zychlinsky A. Neutrophil extracellular traps kill bacteria. Science. 2004;303(5663):1532–1535. doi:10.1126/science.1092385.
2. Urban CF, Reichard U, Brinkmann V, Zychlinsky A. Neutrophil extracellular traps capture and kill *Candida albicans* yeast and hyphal forms. Cell Microbiol. 2006;8(4):668–676. doi:10.1111/j.1462-5822.2005.00659.x.
3. Zawrotniak M, Rapala-Kozik M. Neutrophil extracellular traps (NETs) - formation and implications. Acta Biochim Pol. 2013;60 (3):277–284. doi:10.18388/abp.2013_1983.
4. Papayannopoulos V, Metzler KD, Hakkim A, Zychlinsky A. Neutrophil elastase and myeloperoxidase regulate the formation of neutrophil extracellular traps. J Cell Biol. 2010;191(3):677–691. doi:10.1083/jcb.201006052.
5. Wang Y, Li M, Stadler S, Correll S, Li P, Wang D, Hayama R, Leonelli L, Han H, Grigoryev SA, et al. Histone hypercitrullination mediates chromatin decondensation and neutrophil extracellular trap formation. J Cell Biol. 2009;184(2):205–213. doi:10.1083/jcb.200806072.
6. Clark SR, Ma AC, Tavener SA, McDonald B, Goodarzi Z, Kelly MM, Patel KD, Chakrabarti S, McAvoy E, Sinclair GD, et al. Platelet TLR4 activates neutrophil extracellular traps to ensnare bacteria in septic blood. Nat Med. 2007;13(4):463–469. doi:10.1038/nm1565.
7. Hahn J, Schauer C, Czegley C, Kling L, Petru L, Schmid B, Weidner D, Reinwald C, Biermann MHC, Blunder S, et al. Aggregated neutrophil extracellular traps resolve inflammation by proteolysis of cytokines and chemokines and protection from antiproteases. Faseb J. 2019;33(1):1401–1414. doi:10.1096/fj.201800752R.
8. Lood C, Blanco LP, Purmalek MM, Carmona-Rivera C, De Ravin SS, Smith CK, Malech HL, Ledbetter JA, Elkon KB, Kaplan MJ. Neutrophil extracellular traps enriched in oxidized mitochondrial DNA are interferogenic and contribute to lupus-like disease. Nat Med. 2016;22(2):146–153. doi:10.1038/nm.4027.
9. Lande R, Ganguly D, Facchinetti V, Frasca L, Conrad C, Gregorio J, Meller S, Chamilos G, Sebasigari R, Riccieri V, et al. Neutrophils activate plasmacytoid dendritic cells by releasing self-DNA-peptide complexes in systemic lupus erythematosus. Sci Transl Med. 2011;3(73):73ra19. doi:10.1126/scitranslmed.3001180.
10. Papayannopoulos V. Neutrophil extracellular traps in immunity and disease. Nat Rev Immunol. 2018;18(2):134–147. doi:10.1038/nri.2017.105.
11. Li YW, Qiu SJ, Fan J, Zhou J, Gao Q, Xiao YS, Xu YF. Intratumoral neutrophils: a poor prognostic factor for hepatocellular carcinoma following resection. J Hepatol. 2011;54(3):497–505. doi:10.1016/j.jhep.2010.07.044.
12. Adrover JM, Nicolas-Avila JA, Hidalgo A. Aging: a Temporal Dimension for Neutrophils. Trends Immunol. 2016;37 (5):334–345. doi:10.1016/j.it.2016.03.005.
13. Coffelt SB, Wellenstein MD, de Visser KE. Neutrophils in cancer: neutral no more. Nat Rev Cancer. 2016;16(7):431–446. doi:10.1038/nrc.2016.52.
14. Treffers LW, Hiemstra IH, Kuijpers TW, van den Berg TK, Matlung HL. Neutrophils in cancer. Immunol Rev. 2016;273 (1):312–328. doi:10.1111/imr.12444.
15. Peng ZP, Jiang ZZ, Guo HF, Zhou MM, Huang YF, Ning WR, Huang JH, Zheng L, Wu Y. Glycolytic activation of monocytes regulates the accumulation and function of neutrophils in human hepatocellular carcinoma. J Hepatol. 2020;73(4):906–917. doi:10.1016/j.jhep.2020.05.004.
16. Amulic B, Cazalet C, Hayes GL, Metzler KD, Zychlinsky A. Neutrophil function: from mechanisms to disease. Annu Rev Immunol. 2012;30(1):459–489. doi:10.1146/annurev-immunol-020711-074942.
17. Yang LY, Luo Q, Lu L, Zhu WW, Sun HT, Wei R, Lin ZF, Wang XY, Wang CQ, Lu M, et al. Increased neutrophil extracellular traps promote metastasis potential of hepatocellular carcinoma via provoking tumorous inflammatory response. J Hematol Oncol. 2020;13(1):3. doi:10.1186/s13045-019-0836-0.
18. Yang L, Liu Q, Zhang X, Liu X, Zhou B, Chen J, Huang D, Li J, Li H, Chen F, et al. DNA of neutrophil extracellular traps promotes cancer metastasis via CCDC25. Nature. 2020;583(7814):133–138. doi:10.1038/s41586-020-2394-6.
19. Pieterse E, Rother N, Garsen M, Hofstra JM, Satchell SC, Hoffmann M, Loeven MA, Knaapen HK, van der Heijden OWH, Berden JHM, et al. Neutrophil Extracellular Traps Drive Endothelial-to-Mesenchymal Transition. Arterioscler Thromb Vasc Biol. 2017;37(7):1371–1379. doi:10.1161/atvbaha.117.309002.
20. Ghesquiere B, Wong BW, Kuchnio A, Carmeliet P. Metabolism of stromal and immune cells in health and disease. Nature. 2014;511(7508):167–176. doi:10.1038/nature13312.
21. Biswas SK. Metabolic reprogramming of immune cells in cancer progression. Immunity. 2015;43(3):435–449. doi:10.1016/j.immuni.2015.09.001.
22. Wu C, Ning H, Liu M, Lin J, Luo S, Zhu W, Xu J, Wu WC, Liang J, Shao CK, et al. Spleen mediates a distinct hematopoietic progenitor response supporting tumor-promoting myelopoiesis. J Clin Invest. 2018;128(8):3425–3438. doi:10.1172/JCI97973.
23. Li XF, Chen DP, Ouyang FZ, Chen MM, Wu Y, Kuang DM, Zheng L. Increased autophagy sustains the survival and pro-tumourigenic effects of neutrophils in human hepatocellular carcinoma. J Hepatol. 2015;62(1):131–139. doi:10.1016/j.jhep.2014.08.023.
24. Xu J, Liang J, Meng YM, Yan J, Yu XJ, Liu CQ, Xu L, Zhuang SM, Zheng L. Vascular CXCR4 expression promotes vessel sprouting and sensitivity to sorafenib treatment in hepatocellular carcinoma. Clin Cancer Res. 2017;23(15):4482–4492. doi:10.1158/1078-0432.Ccr-16-2131.

25. Chen DP, Ning WR, Jiang ZZ, Peng ZP, Zhu LY, Zhuang SM, Kuang DM, Zheng L, Wu Y. Glycolytic activation of peritumoral monocytes fosters immune privilege via the PFKFB3-PD-L1 axis in human hepatocellular carcinoma. J Hepatol. 2019;71(2):333–343. doi:10.1016/j.jhep.2019.04.007.
26. Kessenbrock K, Krumbholz M, Schonermarck U, Back W, Gross WL, Werb Z, Grone HJ, Brinkmann V, Jenne DE. Netting neutrophils in autoimmune small-vessel vasculitis. Nat Med. 2009;15(6):623–625. doi:10.1038/nm.1959.
27. Azevedo EP, Rochael NC, Guimaraes-Costa AB, de Souza-vieira TS, Ganilho J, Saraiva EM, Palhano FL, Foguel D. A metabolic shift toward pentose phosphate pathway is necessary for amyloid fibril- and phorbol 12-myristate 13-Acetate-induced Neutrophil Extracellular Trap (NET) Formation. J Biol Chem. 2015;290(36):22174–22183. doi:10.1074/jbc.M115.640094.
28. Fuchs TA, Abed U, Goosmann C, Hurwitz R, Schulze I, Wahn V, Weinrauch Y, Brinkmann V, Zychlinsky A. Novel cell death program leads to neutrophil extracellular traps. J Cell Biol. 2007;176(2):231–241. doi:10.1083/jcb.200606027.
29. Kuang DM, Zhao Q, Wu Y, Peng C, Wang J, Xu Z, Yin XY, Zheng L. Peritumoral neutrophils link inflammatory response to disease progression by fostering angiogenesis in hepatocellular carcinoma. J Hepatol. 2011;54(5):948–955. doi:10.1016/j.jhep.2010.08.041.
30. Wieland E, Rodriguez-Vita J, Liebler SS, Mogler C, Moll I, Herberich SE, Espinet E, Herpel E, Menuchin A, Chang-Claude J, et al. Endothelial notch1 activity facilitates metastasis. Cancer Cell. 2017;31(3):355–367. doi:10.1016/j.ccell.2017.01.007.
31. DeBerardinis RJ, Lum JJ, Hatzivassiliou G, Thompson CB. The biology of cancer: metabolic reprogramming fuels cell growth and proliferation. Cell Metab. 2008;7(1):11–20. doi:10.1016/j.cmet.2007.10.002.
32. van Raam BJ, Verhoeven AJ, Kuijpers TW. Mitochondria in neutrophil apoptosis. Int J Hematol. 2006;84(3):199–204. doi:10.1532/ijh97.06131.
33. Patra KC, Hay N. The pentose phosphate pathway and cancer. Trends Biochem Sci. 2014;39(8):347–354. doi:10.1016/j.tibs.2014.06.005.
34. Fang JH, Zhang ZJ, Shang LR, Luo YW, Lin YF, Yuan Y, Zhuang SM. Hepatoma cell-secreted exosomal microRNA-103 increases vascular permeability and promotes metastasis by targeting junction proteins. Hepatology. 2018;68(4):1459–1475. doi:10.1002/hep.29920.
35. Kuang DM, Peng C, Zhao Q, Wu Y, Zhu LY, Wang J, Yin XY, Li L, Zheng L. Tumor-activated monocytes promote expansion of IL-17-producing CD8+ T cells in hepatocellular carcinoma patients. J Immunol. 2010;185(3):1544–1549. doi:10.4049/jimmunol.0904094.
36. Veglia F, Tyurin VA, Blasi M, De Leo A, Kossenkov AV, Donthireddy L, Tkj T, Schug Z, Basu S, Wang F, et al. Fatty acid transport protein 2 reprograms neutrophils in cancer. Nature. 2019;569(7754):73–78. doi:10.1038/s41586-019-1118-2.